Chemical Science

RSC Publishing

EDGE ARTICLE

View Article Online
View Journal | View Issue

Cite this: *Chem. Sci.*, 2013, **4**, 1234

Long-range metal–ligand bifunctional catalysis: cyclometallated iridium catalysts for the mild and rapid dehydrogenation of formic acid†

Jonathan H. Barnard,[a] Chao Wang,[b] Neil G. Berry[a] and Jianliang Xiao*[a]

Received 6th November 2012
Accepted 19th December 2012

DOI: 10.1039/c2sc21923a

www.rsc.org/chemicalscience

Formic acid (HCO_2H) is an important potential hydrogen storage material, which, in the presence of appropriate catalysts can be selectively dehydrogenated to give H_2 and CO_2. In this work, well defined N^C cyclometallated iridium(III) complexes based on 2-aryl imidazoline ligands are found to be excellent catalysts for the decomposition of HCO_2H–NEt_3 mixtures to give H_2 and CO_2 under mild conditions with high turnover frequencies (up to 147 000 h^{-1} at 40 °C) and essentially no CO formation. The modular structures of these catalysts have allowed for the construction of structure–activity relationships for the complexes, leading to the rational optimisation of the catalyst structure with respect to both the rate of H_2 production and catalyst lifetime. In particular, the presence of the remote γ-NH unit in the ligand is shown to be essential for catalytic activity, without which no reaction occurs. Mechanistic studies suggest that the dehydrogenation is rate-limited by the step of hydride protonation, which is made feasible by the γ-NH unit *via* an unusual form of long-range metal–ligand bifunctional catalysis involving formic acid-assisted proton hopping.

1 Introduction

In the quest for the non-polluting fuels of tomorrow, much attention is directed towards the use of hydrogen.[1] However, despite the high energy density of H_2, its low densities, both in the liquid and compressed gas forms, in conjunction with its high flammability pose considerable barriers to its widespread use.[2] The sequestering of H_2 within stable molecular and supramolecular systems and its subsequent release may overcome these barriers and is an important goal for the realisation of using H_2 as a fuel for transportation. Of these storage media, the use of formic acid (4.4 wt% H_2) is particularly attractive.[3] Formic acid can be obtained by processing biomass,[4] is an easily handled liquid and importantly, the side-product of formic acid dehydrogenation, CO_2, can easily be recycled *via* electrochemical methods[5] or by catalytic hydrogenation,[6] allowing CO_2 to be used as a viable H_2 storage medium. Formic acid may be decomposed *via* a variety of methods, including transition metal catalysed dehydrogenation to H_2 and CO_2[7–13] or by dehydration which is typically promoted by heat or acids.[14] However, if the H_2 is to be used for the generation of electricity, any dehydration is undesirable, as CO impurities are not well tolerated by fuel cells, especially for proton exchange membrane fuel cells.[15]

A variety of transition metal catalysts have been reported for the selective decomposition of HCO_2H to H_2 and CO_2

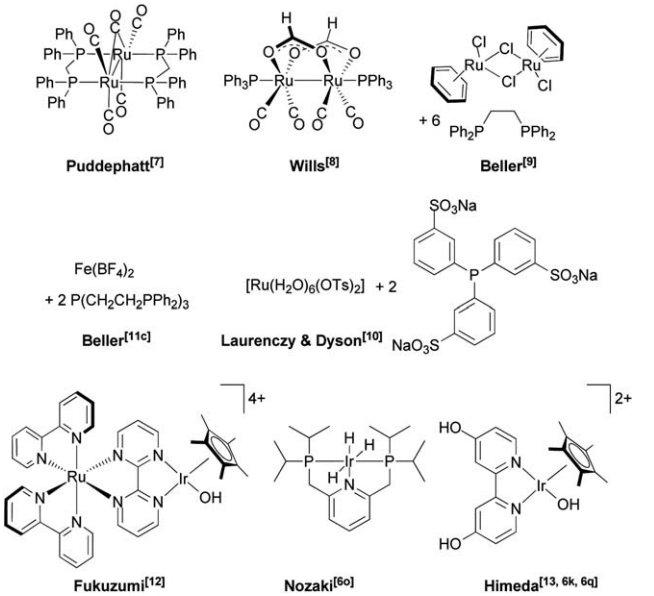

Fig. 1 Homogeneous catalysts for the dehydrogenation of formic acid.

[a]*Department of Chemistry, University of Liverpool, Liverpool, L69 7ZD, UK. E-mail: jxiao@liv.ac.uk; Fax: +44 (0)151-7943588*

[b]*Key Laboratory of Applied Surface and Colloid Chemistry, Ministry of Education, Department of Chemistry & Chemical Engineering, Shaanxi Normal University, Xi'an, 710062, China*

† Electronic supplementary information (ESI) available: Experimental details. CCDC 889583, 889584. For ESI and crystallographic data in CIF or other electronic format see DOI: 10.1039/c2sc21923a

(Fig. 1).[7–13] Puddephatt *et al.*[7] first reported the use of binuclear ruthenium phosphine complexes for formic acid dehydrogenation, achieving a turnover frequency (TOF, mol H_2 per mol catalyst per h) of approximately 500 h^{-1} with $[Ru_2(\mu\text{-}CO)(CO)_4(\mu\text{-}dppm)_2]$ after 0.25 h at room temperature. Later work by Wills *et al.*[8] has detailed the use of binuclear Ru complexes formed *in situ* from $Ru(DMSO)_4Cl_2$ and triphenyl phosphine. Both the groups of Beller[9] and Laurenczy[10] have utilised ruthenium phosphine complexes for the decomposition of HCO_2H. Beller and coworkers also reported a catalyst system composed of $[RuCl_2(benzene)]_2$ and 1,2-bis(diphenylphosphino)ethane which gives high TOFs and turnover numbers (TONs) under the continuous addition of HCO_2H. More recently, the same group reported the use of *in situ* generated iron catalysts,[11] including an Fe(II) tetraphos systems which is active in the absence of amine additives.[11c] Fukuzumi has reported the use of several water-soluble complexes including $[Cp^*Rh(bpy)(H_2O)][SO_4]_2$ and $[Cp^*Ir(H_2O)(bpm)Ru(bpy)_2][SO_4]_4$ for the dehydrogenation of HCO_2H in water, with the latter giving a TOF of 426 h^{-1} under ambient conditions.[12] Himeda *et al.* have reported the use of [Cp*Ir(4,4′-dihydroxy-2,2′-bipyridine)] and related complexes for the dehydrogenation of aqueous HCO_2H–HCOONa solutions with TOFs of up to 228 000 h^{-1} at 90 °C achieved.[6k,6q,13]

Cyclometallated Ru, Rh and Ir complexes[16] have been shown to be excellent catalysts for a range of novel redox processes including amine and alcohol racematisation,[17] dehydrogenation reactions[18] and transfer hydrogenation.[19] Recently, we reported that cyclometallated Cp*IrCl imido complexes derived from acetophenone imines (Fig. 2) are exceptionally active catalysts for the reduction of imines using the 5 : 2 HCO_2H–NEt_3 azeotrope (F/T) as the hydrogen source.[20] During our studies of these and related complexes, we often noted varying degrees of gas evolution. Prompted by these observations and the high modularity of the imido complexes, we were interested as to whether the interception of the Ir–hydride intermediates by protons, rather than iminium cations,[20,21] could lead to fast hydrogen evolution. Herein, we report that a rationally arrived complex shows extremely high activity for formic acid decomposition under mild conditions, and most interestingly, the catalysis involves not only the metal center but also a NH functionality γ to iridium. It appears that H_2 formation is facilitated by HCO_2H-mediated proton hopping.

2 Results and discussion

2.1 Catalyst development

In contrast to the great majority of catalysts for HCO_2H dehydrogenation, the well-defined nature of the cyclometallated complexes, as exemplified in Fig. 2, allows for the detailed and rational development of active catalysts. In particular, the modular structure of these complexes suggested to us that optimisation of each of the constituent parts of the structure, independent of one another, might be possible. To facilitate this, the catalyst structure was considered as four distinct units, *i.e.* the cyclometallated aryl ring, the neutral donor group, the substituents on the donor group and the central metal ion (Fig. 3), which were then examined in greater detail.

2.1.1 Synthesis of initial cyclometallated complexes. A range of [Cp*IrCl(N^C)] complexes (**1–13**) bearing different nitrogen donor groups were first synthesised from their parent ligands (**L1–L13**) (Fig. 4) and $[Cp^*IrCl_2]_2$ *via* the acetate-assisted cyclometallation protocol reported by Davies *et al.*[16a] (eqn (1)). The Ir complexes were formed in good to excellent yields, requiring only simple work up procedures and minimal purification. They also possess excellent stability, necessitating no protection from air or moisture.

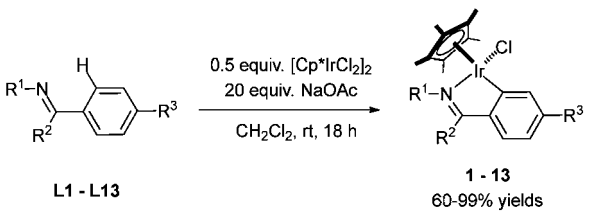

(1)

2.1.2 The effect of the donor group. The complexes **1–13** were then screened as potential catalysts for the decomposition of the 5 : 2 F/T azeotrope at ambient temperature (25 °C). The relative effectiveness of each complex was judged by the comparison of both the initial TOF and the total volume of gas collected in 2 h reaction time (Table 1). As can be seen, HCO_2H dehydrogenation does occur; however, the nature of the donor group has a dramatic effect on the catalytic activity. Complexes with imidamide-based donor groups bearing an NH proton, such as 2-imidazolyl or 2-imidazolinyl, showed good initial TOFs of *ca.* 500–1000 h^{-1} (Table 1, entries 1–5). In stark contrast, complexes bearing other *N*-heterocyclic donors, such as 2-oxazolinyl (precatalyst **6**) or 2-pyridyl (precatalyst **7**), displayed no observable activity at all. Similarly, the use of imine (precatalysts **8–9**) or saturated benzylamine (precatalyst **10**) derived ligands led to a complete loss of activity. No activity was observed when $[Cp^*IrCl_2]_2$ was used, nor did the reaction occur in the absence of any catalyst (entry 8).

Interestingly, replacing the NH proton in the 2-imidazolinyl ligand **L1** with either electron donating (precatalysts **11–12**) or electron withdrawing (precatalyst **13**) substituents led to

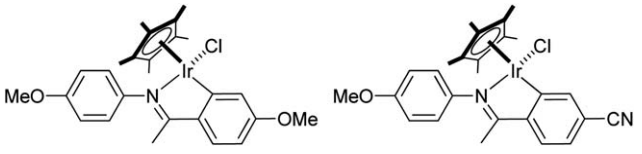

Fig. 2 Cyclometallated Ir(III) complexes used for transfer hydrogenation.

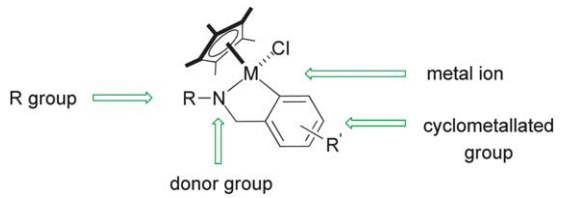

Fig. 3 The modular structure of cyclometallated Cp*MCl complexes.

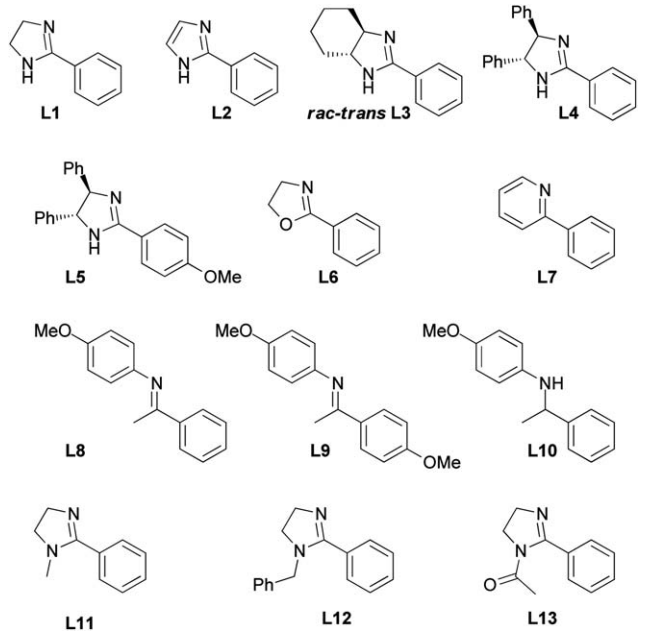

Fig. 4 Ligands examined during initial catalyst development.

Table 1 The effect of ligand structure on the rate of H_2 production[a]

$HCO_2H \xrightarrow[NEt_3,\ 25\ ^oC]{catalyst} H_2 + CO_2$

Entry	Precatalyst	Initial TOF h^{-1}	Vol H_2 (2 h)/mL	TON (2 h)
1	**1**	1090	49	200
2	**2**	536	44.5	182
3	**3**	536	46	188
4	**4**	517	63[c]	258[c]
5	**5**	926	73	298
6	**6–13**	0	0	0
7	$[Cp^*IrCl_2]_2$[b]	0	0	0
8	None	0	0	0

[a] Reactions were performed under an N_2 atmosphere at 25 °C using 10 μmol of catalyst precursor and 1.5 mL of 5 : 2 F/T for 2 h. Initial TOF values were calculated from the volume of gas collected in the first 3 min (see the ESI† for further details). [b] 5 μmol of dimer used. [c] After 1 h.

inactive catalysts, suggesting that the γ-NH functionality plays a critical role in the activity of these catalysts (**1–5**). This is not caused by the steric bulk (or lack of) of the *N*-substituent, as both *N*-methyl and *N*-benzyl complexes were inactive.

The lifetime of the active catalysts appears to depend on the substituents of the donor group. It was noted that during the course of the dehydrogenation reaction, complexes **1–3** (entries 1–3) displayed high initial TOFs; but this activity decreased after *ca.* 0.5 h with an associated darkening of the catalyst solution. However, complexes bearing the bulky 4,5-diphenyl-2-imidazolinyl group (**4** and **5**) displayed prolonged catalytic activity (entries 4 and 5), with no sign of darkening observed even after 2 weeks in neat 5 : 2 F/T solution.

2.1.3 The effect of the cyclometallated group. Modification of the cyclometallated aryl ring in complex **1**, affording pre-catalysts **14–19**, shows that the presence of electron donating substituents *para* to the donor group (*meta* to Ir) enhances the catalytic activity, whilst electron deficient ones severely retard the activity (Table 2).[22] A ρ value of −1.8 was observed in the Hammett plot (Fig. 5), suggesting that positive charge is developed in the transition state of the rate-determining step of the dehydrogenation reaction (*vide infra*). The precatalysts **14–19** were prepared using the ligands **L14–19** under the same conditions as shown in eqn (1).

Among **14–19**, the precatalyst **19**, which bears the 3,4-methylenedioxy disubstituted ligand **L19**, is most active. Having two electron-donating groups, complex **19** was synthesised in an attempt to further enhance the rate of H_2 formation. In the reaction of **L19** with $[Cp^*IrCl_2]_2$, the cyclometallation occurred solely on the 2-position, affording complex **19**. Since the imidazolinyl group and the iridium are each in direct conjugation to the electron-donating *O*-alkyl substituent (Fig. 6), the result, alongside those above, suggests that the dehydrogenation reaction benefits from an electron rich iridium centre.

2.1.4 The effect of the metal ion. In addition to the Cp*IrCl complexes **1–19**, the rhodium analogue **Rh1** was prepared[16a] from **L1** and $[Cp^*RhCl_2]_2$ and its structure confirmed by X-ray crystallographic analysis (see the ESI†). The synthesis of the Ru(η^6−*p*-cymene)Cl analogue was attempted but proved unsuccessful. Comparison of **1** and **Rh1** in the dehydrogenation reaction shows that **Rh1** is not stable under the reaction conditions, with rapid catalyst decomposition and negligible activity observed.

2.1.5 Arriving at the optimal catalyst. In our initial screening, complex **4** and the related **5** proved to be the two most active of those screened (Table 1). However, analysis by ^1H NMR spectroscopy showed them both to be inseparable mixtures of two regioisomers **4a/4b** and **5a/5b**,[23] resulting from competing cyclometallation of the C_2 and C_4 phenyl rings in the NaOAc-mediated cyclometallation reaction (eqn (2)).[16a]

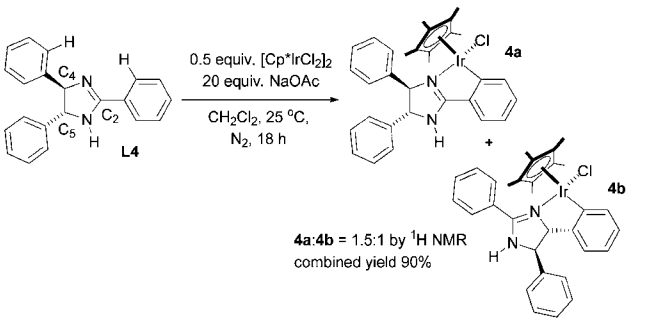

(2)

To gain insight into the relative catalytic activities of these isomers, model compounds were synthesised in order to mimic the selective cyclometallation at the C_2 and C_4 phenyl rings of **L4**. Attempts to synthesise the analogue of **4** with a mesityl group at the C_2 position failed due to an unexpected benzylic sp^3 cyclometallation of the mesityl methyl group. We then

Table 2 The effect of differing *para*-substituents on rate of H_2 production by analogues of **1**[a]

Entry	Ligand	Precatalyst	Initial TOF h^{-1}	Vol H_2 (2 h)/mL	TON (2 h)
1	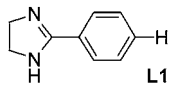 L1	**1**	1090	49	200
2	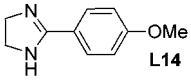 L14	**14**	1690	76.5	312
3	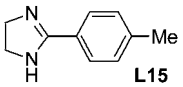 L15	**15**	1390	30	122
4	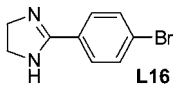 L16	**16**	460	47	192
5	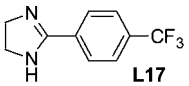 L17	**17**	110	3	12
6	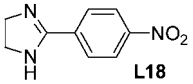 L18	**18**	30	1	4
7	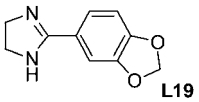 L19	**19**	1960	120	490

[a] Reactions were performed under an N_2 atmosphere at 25 °C using 10 μmol of catalyst precursor and 1.5 mL of 5 : 2 F/T for 2 h. Initial TOF values were calculated as for Table 1.

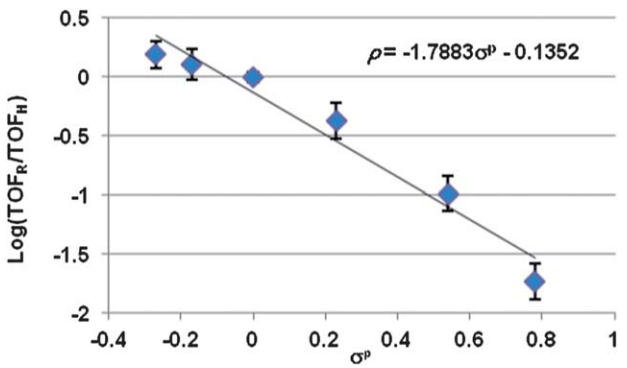

Fig. 5 Hammett plot for substituents *para* to the donor group based on initial TOFs. Reactions were performed under an N_2 atmosphere at 25 °C using 10 μmol of precatalyst and 1.5 mL of 5 : 2 F/T. Data points are an average of 3 or 4 measurements. Error bars show the standard deviation from the mean.

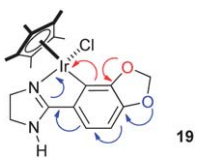

Fig. 6 Conjugation of the bis-alkoxy substituent to the Ir^{III} centre in **19**.

attempted the cyclometallation of the related (*S*,*S*)-4,5-dimesityl-2-phenyl-imidazoline ligand with $[Cp^*IrCl_2]_2$, which unfortunately displayed a pronounced lack of reactivity, even under prolonged and forcing conditions, preventing the synthesis of the desired iridium complex.[24] However, substitution of the C_2-phenyl group by cyclohexyl allowed for the formation of the desired C_4-cyclometallation product **20** (eqn (3)), whilst the use of 3,5-di-*tert*-butylphenyl groups at the C_4 and C_5 positions (**L21**) resulted in selective cyclometallation on the C_2 phenyl ring to give **21** in high yield (eqn (4)). Most interestingly, comparison of the complexes **20** and **21** showed that **20** exhibited no observable activity for dehydrogenation of 5 : 2 F/T at 25 °C, whilst **21** gave an initial TOF of 980 h^{-1}, far exceeding that of **4**, revealing the importance of cyclometallation position to the catalytic activity.

Armed with the structure activity relationships for each part of the catalyst structure, *i.e.* the R group attached to the NH-bearing dative ligand, the dative ligand group L, the cyclometallated aryl ring and the metal ion (see Fig. 3), we reasoned that the combination of the optimised structures of each of the individual subunits would lead to an "optimised" precatalyst structure, **22**, with the key features shown in eqn (5). Synthesis of complex **22** was achieved again using the method of Davies *et al.*[16a] and the structure was unambiguously determined by a combination of multinuclear NMR, HRMS and single crystal X-ray diffraction studies (Fig. 7). As with complex **19**,

cyclometallation occurred selectively at the more hindered position *ortho* to the oxygen substituent.

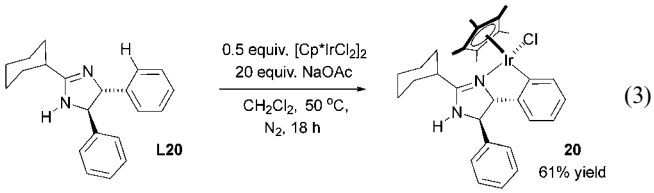

(3)

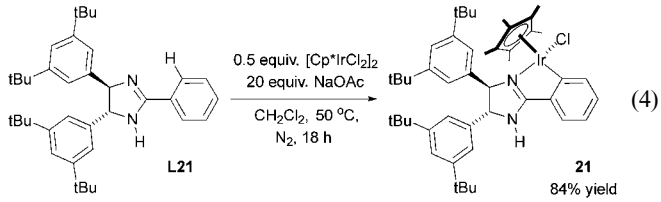

(4)

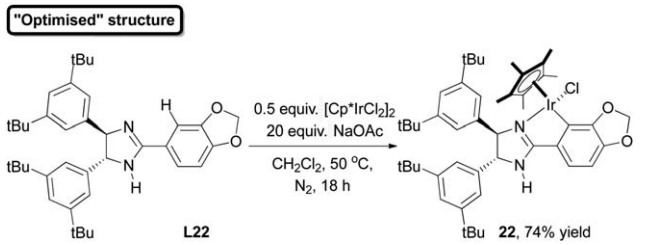

(5)

Gratifyingly, complex **22** indeed showed the highest activity of any of the precatalysts examined in the dehydrogenation of 5 : 2 F/T at 25 °C, with the initial TOF being 2570 h^{-1} under the conditions given in Table 1. GC and ^1H NMR analysis of the gas evolved confirmed the formation of H_2, while analysis with FT-IR showed that the gas is essentially free of CO (see ESI†), which is crucial for its use in fuel cells that are often poorly tolerant of CO.[15] A comparison of the activities of **4**, **20**, **21**, and **22** is shown in Fig. 8. In particular, the initial TOF of **22** is 5 times that of **4**, the starting point of our optimisation process. We noted, however, that the rate of dehydrogenation decreases with time.

2.2 Continuous dehydrogenation of formic acid

In contrast to complex **1**, the more bulky complexes **4**, **5**, **21** and **22** show excellent stability in neat 5 : 2 F/T. Solutions stored under N_2 remained a bright yellow colour for up to 2 weeks and maintained their catalytic activities (if recharged with added HCO_2H). Thus, the decrease in the rates observed with time (Fig. 8) may stem from the consumption of formic acid. Reasoning that the reaction could be slowed by a decrease in formic acid concentration as the reaction progresses and/or possible coordination of NEt_3 to the single active site, we explored further reactions with **22** at 40 °C, in which the catalytic system was recharged by addition of fresh formic acid at regular intervals. Fig. 9 shows that the catalyst indeed maintains its activity if more formic acid is added; without this the dehydrogenation becomes slower after a few minutes.

To further demonstrate the durability of the catalyst, fresh formic acid was added over a period of 2 h (Fig. 10). This allowed high TOFs to be observed, with average TOF = 3080 h^{-1} over the first 1 h and 3340 h^{-1} over 2 h, and the catalyst showed no apparent decrease in the rate of H_2 formation. The almost linear dependence of the H_2 volume on time shows the superb stability of the catalyst and indicates that the dehydrogenation is not rate-limited by the formation of Ir–H hydride under the recharging conditions or at high [HCO_2H] (*vide infra*).

During the course of studying the continuous dehydrogenation of formic acid, it was noted that exceptionally high activity was observed immediately after (1–2 minutes) the reaction was recharged with additional formic acid. For example, addition of 0.1 mL of neat formic acid to a mixture of

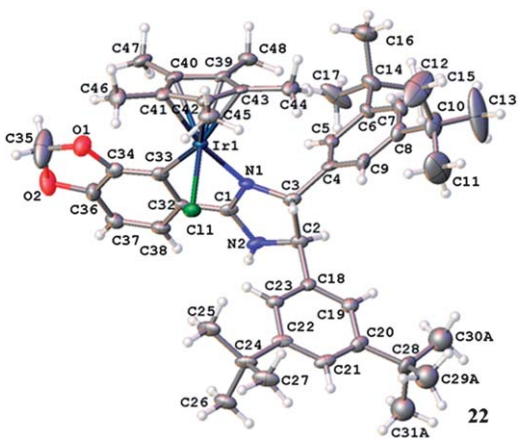

Fig. 7 X-ray structure of **22**. Thermal ellipsoids are drawn at 50% probability. A molecule of *n*-hexane is omitted for clarity and the disorder of a *t*-butyl group (C28, C29, C30, C31) is not shown.

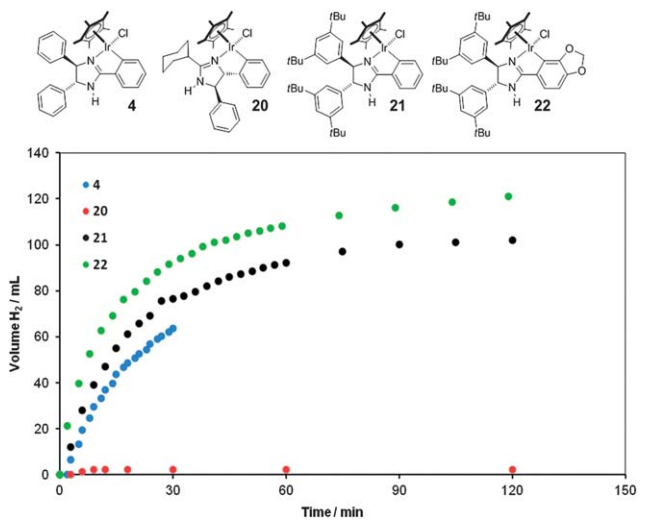

Fig. 8 The effect of cyclometallation position and ligand structure on catalytic activity. Reactions were performed under an N_2 atmosphere at 25 °C using 10 μmol of precatalyst and 1.5 mL of 5 : 2 F/T. For clarity only the major regisomer of complex **4** is shown (regioisomer **4a**).

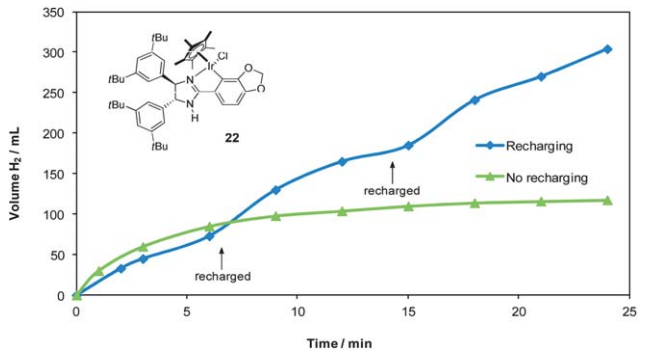

Fig. 9 Comparison of the dehydrogenation of 5 : 2 F/T by **22** with and without HCO_2H recharging (0.05 mL of formic acid at 7.5 min intervals). Reactions were performed under an N_2 atmosphere at 40 °C using 10 μmol of precatalyst and initiated with 1.5 mL of 5 : 2 F/T.

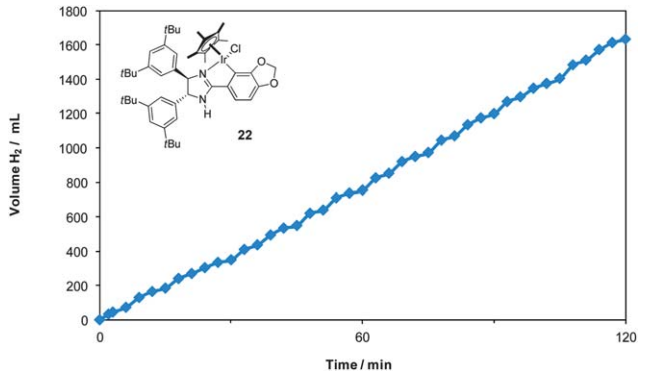

Fig. 10 Dehydrogenation of 5 : 2 F/T by **22** with HCO_2H recharging (0.05 mL of formic acid at 7.5 min intervals). Reactions were performed under an N_2 atmosphere at 40 °C using 10 μmol of precatalyst and initiated with 1.5 mL of 5 : 2 F/T.

10 μmol of **22** in 1.5 mL of azeotrope at 40 °C led to a large increase in rate, with the reproducible formation of 100 mL of gas within 60 s, corresponding to a TOF of 24 500 h^{-1} for that period. Even more dramatic was the addition of 0.5 mL of neat formic acid to an identical mixture, which led to the reproducible formation of 100 mL of gas within 10 s, corresponding to a TOF of 147 000 h^{-1} for that period (see ESI† for the calculations). However, as the additional formic acid was consumed the rate of gas evolution returned to the previous level. These results suggest that formic acid is likely to be involved in the rate-determined step of the dehydrogenation. It must be noted, however, that the addition of formic acid to solutions of F/T containing inactive complexes, or no catalyst, did not result in any gas evolution.

2.3 Mechanism of H_2 formation

2.3.1 Formation of hydrides. The high catalytic activity of **22** and other complexes bearing an N=C–NH unit, and the lack of activity of closely related complexes without this structural feature prompted us to investigate the mechanism of H_2 formation and the role of the apparently crucial remote NH functionality. Initially we examined hydride formation using **1** as a simplified model of complex **22**. As in transfer hydrogenation reactions using 5 : 2 F/T as the H_2 source, coordination of formate to the metal centre and subsequent β-hydride elimination furnishes the metal hydride and CO_2.[25] This was demonstrated by stoichiometric reactions of **1** with tetra-*n*-butylammonium formate[26] in CD_3CN at room temperature to give solutions of the corresponding hydride complex **23** (eqn (6)). Alternatively, **23** could be obtained as a pure solid by reaction of **1** with sodium formate in a biphasic DCM–water mixture with tetra-*n*-butylammonium formate as a phase transfer catalyst (see ESI†). Complex **23** showed a single resonance in the hydride region (δ −15.5 ppm) and an NH resonance (δ 5.8 ppm) and remained stable both in the solid state and in solution (CD_3CN) for prolonged periods (>3 days, N_2, rt). The long-lived nature of **23** in the absence of exogenous acid is at odds with the rapid H_2 evolution observed under catalytic conditions, suggesting that spontaneous formation of H_2, *via*, for example, long distance protonation of the hydride by the NH proton, does not occur from this species alone.

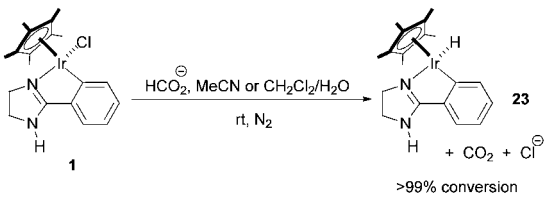

(6)

When **1** or **23** was treated with an excess of 5 : 2 F/T in CD_3CN at ambient temperature, visible H_2 evolution occurred. Analysis of the Cp*, aliphatic and aromatic regions of the ^1H NMR spectrum of the solution showed no peaks other than those corresponding to **23**, F/T or H_2, showing **23** to be both a plausible intermediate in the catalytic cycle and the catalyst resting state. The latter is consistent with the dehydrogenation not being controlled by hydride formation and suggests H_2 formation to be the rate limiting step. A small second hydride peak (<10%) was also observed but NOESY experiments showed no correlations between it and any other proton resonances. In addition, it does not appear to be derived from the $[Cp^*IrCl_2]_2$ dimer or breakdown Cp*Ir products,[27] consistent with the clean high-field ^1H NMR spectrum of **23** obtained under catalytic conditions. As yet, the identity of this minor species is unknown.

Notably, the NH proton of **23** was not observed in the ^1H NMR spectrum under the catalytic conditions. Similarly, the addition of soluble acetate or dimethylphosphate salts to pure solutions of **23** in CD_3CN led to the disappearance of its NH proton in the ^1H NMR spectrum (see the ESI†, Section 3.3). This is most likely a result of the NH unit engaging in hydrogen bonding with the oxygen anions, suggesting that under catalytic conditions, **23** hydrogen-bonds with formate. However, the NH resonance remained unchanged when the neutral hydrogen bond acceptors NEt_3 or methyl 4-methoxybenzoate were added to pure solutions of **23** in CD_3CN.

2.3.2 Reactions of hydrides. In order to gain insight into the mechanism of H_2 formation, the reactivity of **23** was further

investigated. In addition, the closely related hydride **24**, which was readily formed from complex **6** (as with the case of **23** from **1**), was studied for comparison (Fig. 11), as its precursor **6** had been shown to be inactive for H_2 formation. Both hydride complexes were found to be stable in dry CD_3CN or in the presence of added H_2O for prolonged periods of time (>3 days, N_2, rt). Addition of a slight excess of HOAc or 1 equivalent of $Ph_3CCH_2CO_2H$ to solutions of **23** led to the instant disappearance of the hydride resonance and the formation of H_2, as observed by ^1H NMR spectroscopy. In sharp contrast, no reaction occurred with **24** (Fig. 11). As both **23** and **24** are formed rapidly when their parent chlorides are treated with formate, this suggests that the feasibility of protonation of the hydride to form H_2 may explain the differing reactivities of **1** and **6** for formic acid dehydrogenation.

The NH functionality is crucial for any observable activity in both the hydride protonation reaction and catalytic H_2 formation. As substituting the NH for electron-donating (NMe, NBn) and electron-withdrawing groups (NAc) or oxygen results in a total loss of catalyst activity (Table 1), the effects conferred by the NH unit must stem from the presence of the proton on nitrogen, rather than any steric or electronic effects. Thus, any potential mechanism in which the Ir–hydride complex is directly protonated without involvement of the NH unit would appear to be unlikely.

The structure of the acid was also found to be crucial. Whilst carboxylic acids rapidly protonated **23**, despite their exceedingly low acidities in anhydrous MeCN,[28] other Brønsted acids did not. Thus, despite possessing acidities close to, or greater than, that of acetic acid in MeCN, no reaction was observed between either 2-nitrophenol, 4-cyanophenol or 9-fluorene-9-carboxylic acid methyl ester and either **23** or **24**, showing that both the structure of the acid and the hydride are crucial for efficient H_2 formation. On the other hand, both **23** and **24** could be protonated with either triphenylphosphonium tetrafluoroborate[29] or 2,6-lutidinium tetrafluoroborate[30] to release H_2 and form the phosphine and MeCN ligated cationic species, respectively (Fig. 11). However, it must be noted that triphenylphosphonium and 2,6-lutidinium are approximately 16 and 9 pK_a units more acidic than HOAc and related carboxylic acids in MeCN, respectively.[28] These results show that whilst both hydrides **23** and **24** can be protonated with strong acids, they display a distinct difference in their reactivity toward carboxylic acids, providing an explanation as to why **23** is active, whilst **24** is not, in the dehydrogenation of HCOOH.

2.3.3 Mechanistic possibilities. Bearing in mind the importance of the NH functionality and the carboxylic acid to H_2 formation, which hydrogen-bond with each other under catalytic conditions, we considered the two following possibilities for hydride protonation:

(1) Analogous to the Grotthuss mechanism[31] for proton transfer in H_2O and biological systems, formic acid could participate in a proton-hopping process, hydrogen-bonding to the NH proton while enabling protonation of the hydride. Two pathways could be envisioned, one involving transfer of the formic acid proton directly to the hydride *via* one or more molecules of hydrogen-bonding formic acid to generate a dihydrogen complex **25** (eqn (7)), and the other involving an initial proton transfer to the iridium-bound nitrogen, forming **27**, followed by H_2 formation *via* a Noyori type mechanism[32] (eqn (8)). In both cases, the proton from the distal nitrogen is transferred, regenerating the formic acid. Subsequent loss of H_2 and addition of formic acid would result in the protonation of the distal nitrogen and formation of a metal formato complex **26**, which regenerates the hydride **23** upon decarboxylation. Studies by Casey and coworkers on the mechanism of H_2 loss from $[(2,5\text{-}Ph_2\text{-}3,4\text{-}Tol_2(\eta^5\text{-}C_4COH))Ru(CO)_2H]$ at high temperatures have highlighted the role of H_2O or alcohols in catalysing the transfer of the acidic proton to the hydride to form a dihydrogen complex, which subsequently releases H_2.[33]

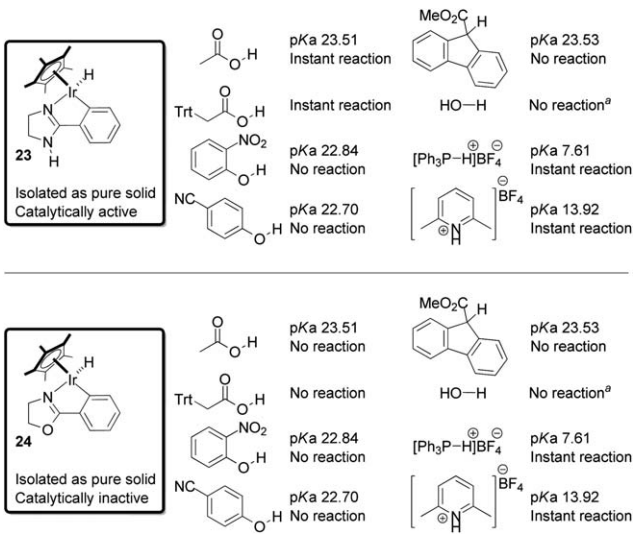

Fig. 11 Reactions of **23** and **24** with a variety of proton sources. Unless specified, reactions were performed under N_2 with 1.0 equivalent of the acid in anhydrous CD_3CN at room temperature. pK_a's given are in MeCN.[28]; [a]Excess H_2O was used. Trt is trityl (triphenylmethyl).

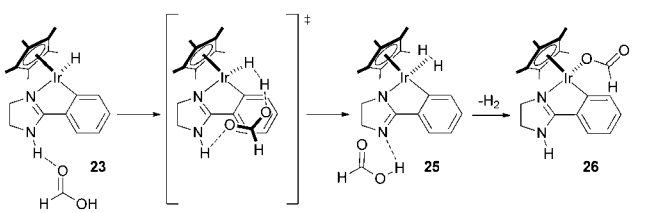

(7)

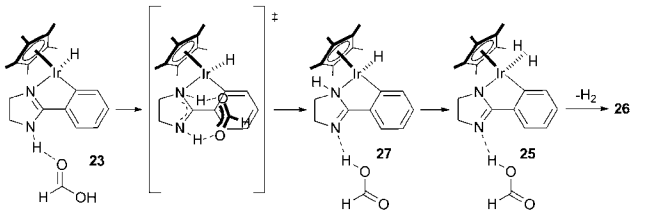

(8)

The formation of **26** is likely to involve the intermediacy of a neutral 16-electron species generated from H_2 dissociation from **25**. This species, **28**, was observed by ^{1}H NMR on reacting **1** with 1.05 equivalents of potassium *tert*-butoxide in anhydrous CD_3CN, along with a colour change from bright yellow to deep red/brown (eqn (9)). Interestingly, treatment of **28** with hydrogen in CD_3CN led to the ready formation of **23** in the absence of a carboxylic acid. The analogous reaction with triphenylphosphonium tetrafluoroborate gave the phosphine ligated cation (eqn (10)), which was confirmed by its independent synthesis (*vide supra*), thus supporting the identity of **28**. The fact that **23** can be generated from **28** *via* hydrogenation lends support to the pathway shown in eqn (8), as the hydrogenation is expected to proceed *via* the intermediacy of **25** and then **27**, *i.e.* the reverse reaction of H_2 formation (eqn (8)). Hydrogenation of related neutral complexes bearing a basic amide ligand with H_2 to generate metal hydrides is known, albeit slow, as shown by the work of Noyori, Ikariya and Rauchfuss.[34] Although long-range activation of H_2 by the Ir and distal N atom cannot be ruled out,[35] the stability of **23** is at odds with this possibility.

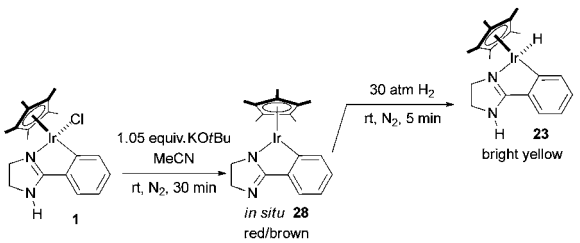

(9)

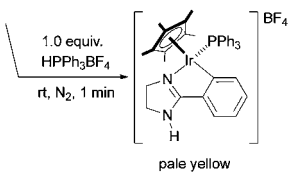

(10)

(2) As the NH proton is strongly hydrogen bonded under catalytic conditions, it was considered that this hydrogen bonding of the NH proton could increase the electron density at the Ir centre, imparting increased hydricity to the hydride ligand and thus aiding its intermolecular protonation by formic acid. This is a process which may be considered analogous to that operational in the catalytic triad present in trypsin and similar proteases, in which hydrogen bonding of an aspartate residue to a histidine residue increases the basicity (electron density) of the histidine imidazole, allowing it to activate a nearby serine as a powerful nucleophile.[36]

To investigate whether hydrogen bonding between **23** and formate could play a role in the hydrogen forming step under catalytic conditions, CD_3CN solutions of **23** were first treated with a slight excess of dimethylimidazolium dimethylphosphate or tetra-*n*-butylammonium acetate. Hydrogen bonding to the NH proton of **23** was indicated by the disappearance of the NH resonance,[37] although the hydride resonance remained unchanged. However, addition of 1 equivalent of 4-cyanophenol (see also Fig. 11) to this solution did not result in the loss of the hydride signal or the formation of hydrogen, as observed by ^{1}H NMR, even after 24 h. Although the protonation of **23** by carboxylic acids may be more favourable than with phenols or carbon-based acids due to the intermediacy of 4-membered transition states in the latter cases, the ability of carboxylic acids to protonate **23** in the absence of any additives makes an acid-assisted proton transfer pathway a more likely one, in particular eqn (8).

Taken together, we tentatively suggest that the catalytic dehydrogenation of formic acid by **22** and related complexes proceeds *via* the mechanism shown in Fig. 12. The key feature of the mechanism is that the catalytic turnover is rate-limited by the protonation of the Ir–H hydride, which is the resting state of the catalyst, and that its protonation involves participation of both formic acid and the distal NH functionality, without which catalysis does not occur. Most likely, the protonation proceeds *via* formic acid-assisted proton hopping from the distal to the proximal nitrogen, whereupon protonation takes place, forming the dihydrogen complex and eventually H_2.

3 Conclusions

This study shows that well defined bifunctional Cp*IrCl(N^C) complexes containing cyclometallated 2-aryl-imidazoline ligands are excellent precatalysts for the dehydrogenation of azeotropic HCO_2H–NEt_3 mixtures, producing H_2 and CO_2 with high turnover rates under exceptionally mild conditions. In contrast to most other systems for this process, the modular nature of the catalyst precursors allowed for the independent optimisation of the constituent "modules", which when

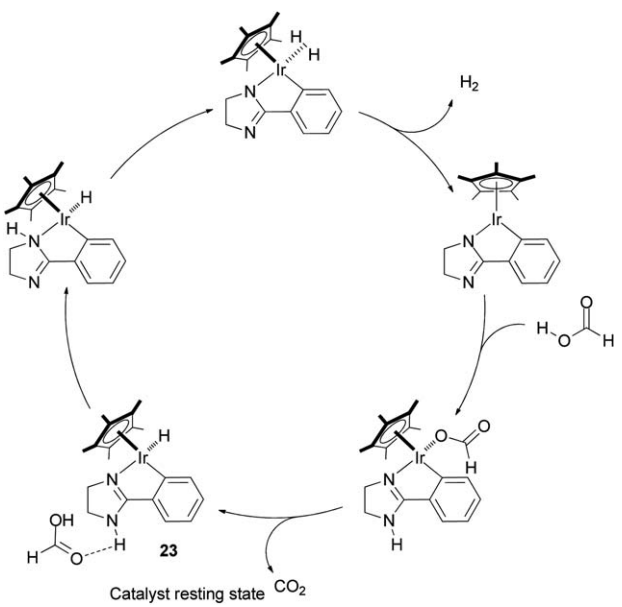

Fig. 12 Proposed catalytic cycle for the dehydrogenation of HCO_2H.

combined, led to a rationally designed "optimal" metal–ligand bifunctional catalyst that showed excellent activity, outperforming all its predecessors.

Evidence is provided, which shows that the remote NH functionality is crucial to the catalysis, without which there is no dehydrogenation, and suggests that formic acid plays a dual role, acting both as a hydride and a proton source and as a proton shuttle. The NH proton does not directly protonate the Ir–H hydride, nor does formic acid. Instead, a formic acid assisted-proton hopping may occur, resulting in proton transfer from the remote to the proximal nitrogen atom, whereupon protonation of the hydride and subsequent release of H_2 takes place. This process constitutes a rare example of bifunctional catalysis, in which unusual long-range metal–ligand cooperation effects the catalysis through a conventional "short-range" metal–ligand bifunctional mechanism. Further studies of hydrogen release from these bifunctional catalysts and applications in hydrogen transfer reactions and H_2 formation from other substrates will be reported in due course.

Acknowledgements

We thank the University of Liverpool for support, Dr John Bacsa for X-ray structural analysis and the EPSRC National Mass Spectrometry Service Centre for mass analysis.

Notes and references

1 (*a*) N. S. Lewis and D. Nocera, *Proc. Natl. Acad. Sci. U. S. A.*, 2006, **103**, 15729; (*b*) J. A. Turner, *Science*, 1999, **285**, 687; (*c*) J. A. Turner, *Science*, 2004, **305**, 972.

2 (*a*) L. Schlapbach and A. Zuttel, *Nature*, 2001, **414**, 353; (*b*) S. Fukuzumi, *Eur. J. Inorg. Chem.*, 2008, 1351; (*c*) P. Makowski, A. Thomas, P. Kuhn and F. Goettmann, *Energy Environ. Sci.*, 2009, **2**, 480.

3 (*a*) F. Joó, *ChemSusChem*, 2008, **1**, 805; (*b*) S. Enthaler, *ChemSusChem*, 2008, **1**, 801; (*c*) B. Loges, A. Boddien, F. Gärtner, H. Junge and M. Beller, *Top. Catal.*, 2010, **53**, 902; (*d*) T. C. Johnson, D. J. Morris and M. Wills, *Chem. Soc. Rev.*, 2010, **39**, 81; (*e*) H.-L. Jiang, S. K. Singh, J.-M. Yan, X.-B. Zhang and Q. Xu, *ChemSusChem*, 2010, **3**, 541; (*f*) M. Grasemann and G. Laurenczy, *Energy Environ. Sci.*, 2012, **5**, 8171.

4 F. Jin, J. Yun, G. Li, A. Kishita, K. Tohji and H. Enomoto, *Green Chem.*, 2008, **10**, 612.

5 (*a*) E. E. Benson, C. P. Kubiak, A. J. Sathrum and J. M. Smieja, *Chem. Soc. Rev.*, 2009, **38**, 89; (*b*) H. Arakawa, M. Aresta, J. N. Armor, M. A. Barteau, E. J. Beckman, A. T. Bell, J. E. Bercaw, C. Creutz, E. Dinjus, D. A. Dixon, K. Domen, D. L. DuBois, J. Eckert, E. Fujita, D. H. Gibson, W. A. Goddard, D. W. Goodman, J. Keller, G. J. Kubas, H. H. Kung, J. E. Lyons, L. E. Manzer, T. J. Marks, K. Morokuma, K. M. Nicholas, R. Periana, L. Que Jr, J. Rostrup-Nielson, W. M. H. Sachtler, L. D. Schmidt, A. Sen, G. A. Somorjai, P. C. Stair, B. R. Stults and W. Tumas, *Chem. Rev.*, 2001, **101**, 953.

6 (*a*) P. G. Jessop, T. Ikariya and R. Noyori, *Nature*, 1994, **368**, 231; (*b*) P. G. Jessop, Y. Hsiao, T. Ikariya and R. Noyori, *J. Am. Chem. Soc.*, 1996, **118**, 344; (*c*) P. Munshi, A. D. Main, J. C. Linehan, C. C. Tai and P. G. Jessop, *J. Am. Chem. Soc.*, 2002, **124**, 7963; (*d*) P. G. Jessop, in *The Handbook of Homogeneous Hydrogenation*, ed. J. G. de Vries and C. J. Elsevier, Wiley-VCH, Weinheim, 2007, p. 489; (*e*) G. Laurenczy, F. Joo and L. Nadasdi, *Inorg. Chem.*, 2000, **39**, 5083; (*f*) C. Q. Yin, Z. T. Xu, S. Y. Yang, S. M. Ng, K. Y. Wong, Z. Y. Lin and C. P. Lau, *Organometallics*, 2001, **20**, 1216; (*g*) C. C. Tai, J. Pitts, J. C. Linehan, A. D. Main, P. Munshi and P. G. Jessop, *Inorg. Chem.*, 2002, **41**, 1606; (*h*) Y. Y. Ohnishi, T. Matsunaga, Y. Nakao, H. Sato and S. Sakaki, *J. Am. Chem. Soc.*, 2005, **127**, 4021; (*i*) A. Urakawa, F. Jutz, G. Laurenczy and A. Baiker, *Chem.–Eur. J.*, 2007, **13**, 3886; (*j*) S. Ogo, R. Kabe, H. Hayashi, R. Harada and S. Fukuzumi, *Dalton Trans.*, 2006, 4657; (*k*) Y. Himeda, N. Onozawa-Komatsuzaki, H. Sugihara and K. Kasuga, *Organometallics*, 2007, **26**, 702; (*l*) R. Tanaka, M. Yamashita and K. Nozaki, *J. Am. Chem. Soc.*, 2009, **131**, 14168; (*m*) C. Federsel, A. Boddien, R. Jackstell, R. Jennerjahn, P. J. Dyson, R. Scopelliti, G. Laurenczy and M. Beller, *Angew. Chem., Int. Ed.*, 2010, **49**, 9777; (*n*) D. Preti, C. Resta, S. Squarcialupi and G. Fachinetti, *Angew. Chem., Int. Ed.*, 2011, **50**, 12551; (*o*) R. Tanaka, M. Yamashita, L. W. Chung, K. Morokuma and K. Nozaki, *Organometallics*, 2011, **30**, 6724; (*p*) T. J. Schmeier, G. E. Dobereiner, R. H. Crabtree and N. Hazari, *J. Am. Chem. Soc.*, 2011, **133**, 9274; (*q*) J. F. Hull, Y. Himeda, W.-H. Wang, B. Hashiguchi, R. Periana, D. J. Szalda, J. T. Muckerman and E. Fujita, *Nat. Chem.*, 2012, **4**, 383.

7 (*a*) Y. Gao, J. Kuncheria, R. J. Puddephatt and G. P. A. Yap, *Chem. Commun.*, 1998, 2365; (*b*) Y. Gao, J. K. Kuncheria, H. A. Jenkins, R. J. Puddephatt and G. P. A. Yap, *J. Chem. Soc., Dalton Trans.*, 2000, 3212.

8 (*a*) D. J. Morris, G. J. Clarkson and M. Wills, *Organometallics*, 2009, **28**, 4133; (*b*) A. Majewski, D. J. Morris, K. Kendall and M. Wills, *ChemSusChem*, 2010, **3**, 431.

9 (*a*) B. Loges, A. Boddien, H. Junge and M. Beller, *Angew. Chem., Int. Ed.*, 2008, **47**, 3962; (*b*) A. Boddien, B. Loges, H. Junge and M. Beller, *ChemSusChem*, 2008, **1**, 751; (*c*) H. Junge, A. Boddien, F. Capitta, B. Loges, J. R. Noyes, S. Gladiali and M. Beller, *Tetrahedron Lett.*, 2009, **50**, 1603; (*d*) A. Boddien, B. Loges, H. Junge, F. Gärtner, J. R. Noyes and M. Beller, *Adv. Synth. Catal.*, 2009, **351**, 2517; (*e*) A. Boddien, F. Gärtner, C. Federsel, P. Sponholz, D. Mellmann, R. Jackstell, H. Junge and M. Beller, *Angew. Chem., Int. Ed.*, 2011, **50**, 6411.

10 (*a*) C. Fellay, P. J. Dyson and G. Laurenczy, *Angew. Chem., Int. Ed.*, 2008, **47**, 3966; (*b*) C. Fellay, N. Yan, P. J. Dyson and G. Laurenczy, *Chem.–Eur. J.*, 2009, **15**, 3752; (*c*) W. Gan, P. J. Dyson and G. Laurenczy, *React. Kinet. Catal. Lett.*, 2009, **98**, 205; (*d*) G. Papp, J. Csorba, G. Laurenczy and F. Joó, *Angew. Chem., Int. Ed.*, 2011, **50**, 10433.

11 (*a*) A. Boddien, B. Loges, F. Gärtner, C. Torborg, K. Fumino, H. Junge, R. Ludwig and M. Beller, *J. Am. Chem. Soc.*, 2010, **132**, 8924; (*b*) A. Boddien, F. Gärtner, R. Jackstell, H. Junge,

A. Spannenberg, W. Baumann, R. Ludwig and M. Beller, *Angew. Chem., Int. Ed.*, 2010, **49**, 8993; (*c*) A. Boddien, D. Mellmann, F. Gärtner, R. Jackstell, H. Junge, P. J. Dyson, G. Laurenczy, R. Ludwig and M. Beller, *Science*, 2011, **333**, 1733.

12 (*a*) S. Fukuzumi, T. Kobayashi and T. Suenobu, *ChemSusChem*, 2008, **1**, 827; (*b*) S. Fukuzumi, T. Kobayashi and T. Suenobu, *J. Am. Chem. Soc.*, 2010, **132**, 1496; (*c*) Y. Maenaka, T. Suenobu and S. Fukuzumi, *Energy Environ. Sci.*, 2012, **5**, 7360.

13 (*a*) Y. Himeda, *Green Chem.*, 2009, **11**, 2018; (*b*) Y. Himeda, S. Miyazawa and T. Hirose, *ChemSusChem*, 2011, **4**, 487.

14 (*a*) H. Koch and W. Haaf, *Org. Synth.*, 1973, **5**, 20; (*b*) G. H. Coleman and D. Craig, *Org. Synth.*, 1943, **2**, 583.

15 J. J. Baschuk and X. Li, *Int. J. Energy Res.*, 2001, **25**, 695.

16 (*a*) D. L. Davies, O. Al-Duaij, J. Fawcett, M. Giardiello, S. T. Hilton and D. R. Russell, *Dalton Trans.*, 2003, 4132; (*b*) D. L. Davies, S. M. A. Donald, O. Al-Duaij, S. A. Macgregor and M. Pölleth, *J. Am. Chem. Soc.*, 2006, **128**, 4210; (*c*) Y. Boutadla, D. L. Davies, R. C. Jones and K. Singh, *Chem.–Eur. J.*, 2011, **17**, 3438; (*d*) L. Li, W. W. Brennessel and W. D. Jones, *Organometallics*, 2009, **28**, 3492; (*e*) M. E. van der Boom and D. Milstein, *Chem. Rev.*, 2003, **103**, 1759.

17 (*a*) T. Jerphagnon, A. J. A. Gayet, F. Berthiol, V. Ritleng, N. Mršić, A. Meetsma, M. Pfeffer, A. J. Minnaard, B. L. Feringa and J. G. de Vries, *Chem.–Eur. J.*, 2009, **15**, 12780; (*b*) S. Arita, T. Koike, Y. Kayaki and T. Ikariya, *Angew. Chem., Int. Ed.*, 2008, **47**, 2447; (*c*) S. Arita, T. Koike, Y. Kayaki and T. Ikariya, *Organometallics*, 2008, **27**, 2795.

18 (*a*) G. E. Dobereiner and R. H. Crabtree, *Chem. Rev.*, 2010, **110**, 681; (*b*) J. Choi, A. H. R. MacArthur, M. Brookhart and A. S. Goldman, *Chem. Rev.*, 2011, **111**, 1761; (*c*) M. Gupta, C. Hagen, R. J. Flesher, W. C. Kaska and C. M. Jensen, *Chem. Commun.*, 1996, 2083; (*d*) M. Gupta, C. Hagen, W. C. Kaska, R. E. Cramer and C. M. Jensen, *J. Am. Chem. Soc.*, 1997, **119**, 840; (*e*) M. Gupta, W. C. Kaska and C. M. Jensen, *Chem. Commun.*, 1997, 461; (*f*) W.-w. Xu, G. P. Rosini, K. Krogh-Jespersen, A. S. Goldman, M. Gupta, C. M. Jensen and W. C. Kaska, *Chem. Commun.*, 1997, 2273; (*g*) F. Liu, E. B. Pak, B. Singh, C. M. Jensen and A. S. Goldman, *J. Am. Chem. Soc.*, 1999, **121**, 4086; (*h*) F. Liu and A. S. Goldman, *Chem. Commun.*, 1999, 655; (*i*) K. Zhu, P. D. Achord, X. Zhang, K. Krogh-Jespersen and A. S. Goldman, *J. Am. Chem. Soc.*, 2004, **126**, 13044; (*j*) G. C. Fortman, A. M. Z. Slawin and S. P. Nolan, *Organometallics*, 2011, **30**, 5487; (*k*) T. W. Graham, C.-W. Tsang, X. Chen, R. Guo, W. Jia, S.-M. Lu, C. Sui-Seng, C. B. Ewart, A. Lough, D. Amaroso and K. Abdur-Rashid, *Angew. Chem., Int. Ed.*, 2010, **49**, 8708.

19 (*a*) J. B. Sortais, V. Ritleng, A. Voelklin, A. Holuigue, H. Smail, L. Barloy, C. Sirlin, G. K. M. Verzijl, J. A. F. Boogers, A. H. M. de Vries, J. G. de Vries and M. Pfeffer, *Org. Lett.*, 2005, **7**, 1247; (*b*) N. Pannetier, J.-B. Sortais, P. S. Dieng, L. Barloy, C. Sirlin and M. Pfeffer, *Organometallics*, 2008, **27**, 5852.

20 (*a*) C. Wang, A. Pettman, J. Basca and J. Xiao, *Angew. Chem., Int. Ed.*, 2010, **49**, 7548; (*b*) J.-X. Jiang, C. Wang, A. Laybourn, T. Hasell, R. Clowes, Y. Z. Khimyak, J. Xiao, S. J. Higgins, D. J. Adams and A. I. Cooper, *Angew. Chem. Int. Ed.*, 2011, **50**, 1072; (*c*) C. Wang, B. Villa-Marcos and J. Xiao, *Chem. Commun.*, 2011, **47**, 9773.

21 (*a*) M. P. Magee and J. R. Norton, *J. Am. Chem. Soc.*, 2001, **123**, 1778; (*b*) H. Guan, M. Iimura, M. P. Magee, J. R. Norton and G. Zhu, *J. Am. Chem. Soc.*, 2005, **127**, 7805; (*c*) J. B. Åberg, J. S. M. Samec and J. E. Bäckvall, *Chem. Commun.*, 2006, 2771.

22 The effect of single substituents *meta* to the donor group (*para* to the Ir centre) could not be thoroughly assessed as the majority of ligands bearing a *meta* substituent gave rise to mixtures of complexes with the substituent *ortho* and *para* to the Ir centre. For reasons as yet unknown, only the methyl substituted ligand gave a single cyclometallation product with the methyl group *para* to the Ir centre. The effect of placing an electron donating methyl substituent *meta* to the donor group (*para* to Ir) was found to be similarly beneficial to the rate of catalysis (initial TOF 1226 h^{-1}) as the presence of a methyl group *para* to the donor group (*meta* to Ir) (initial TOF 1390 h^{-1}).

23 A total of 7 resonances were observed in the case of **4** in the range 5.0–6.5 ppm corresponding to the following: the NH proton, the two methylidyne protons of each of a pair of diastereoisomeric complexes resulting from cyclometallation on the C_2 ring, and the pair of methylidyne protons from the complex resulting from cyclometallation on the C_4 aryl ring.

24 No reaction observed by ^{1}H NMR spectroscopy after 4 days at 40 °C.

25 (*a*) T. Koike and T. Ikariya, *Adv. Synth. Catal.*, 2004, **346**, 37; (*b*) T. Abura, S. Ogo, Y. Watanabe and S. Fukuzumi, *J. Am. Chem. Soc.*, 2003, **125**, 4149; (*c*) N. Makihara, S. Ogo and Y. Watanabe, *Organometallics*, 2001, **20**, 497.

26 See ESI† for details of preparation of tetra-*n*-butylammonium formate.

27 Analysis of the reactions of $[Cp^*IrCl_2]_2$, $[Ir(Cl)COD]_2$ and $IrCl_3 \cdot nH_2O$ with excess 5 : 2 F/T in CD_3CN under the same conditions by ^{1}H NMR spectroscopy did not show resonances which were consistent with that of the minor hydride species (δ −16.33 ppm). In light of this, and the lack of any species that would be derived from the breakdown of **23** (*i.e.* free ligand), the minor hydride species remains unassigned.

28 (*a*) A. Kütt, I. Leito, I. Kaljurand, L. Sooväli, V. M. Vlasov, L. M. Yagupolskii and I. A. Koppel, *J. Org. Chem.*, 2006, **71**, 2829; (*b*) I. Kaljurand, A. Kütt, L. Sooväli, T. Rodima, V. Mäemets, I. Leito and I. A. Koppel, *J. Org. Chem.*, 2005, **70**, 1019.

29 Triphenylphosphonium tetrafluoroborate was prepared using the method described in P. J. C. Hausoul, A. N. Parvulescu, M. Lutz, A. L. Spek, P. C. A. Bruijnincx, B. M. Weckhuysen and R. J. M. K. Gebbink, *Angew. Chem., Int. Ed.*, 2010, **49**, 7972.

30 2,6-Lutidinium tetrafluoroborate was prepared using the method described in F. Santoro, M. Althaus, C. Bonaccorsi, S. Gischig and A. Mezzetti, *Organometallics*, 2008, **27**, 3866.
31 C. J. T. von Grotthuss, *Ann. Chim.*, 1806, **58**, 54.
32 (*a*) T. Ikariya, K. Murata and R. Noyori, *Org. Biomol. Chem.*, 2006, **4**, 393; (*b*) R. Noyori, M. Yamakawa and S. Hashiguchi, *J. Org. Chem.*, 2001, **66**, 7931.
33 C. P. Casey, J. B. Johnson, S. W. Singer and Q. Cui, *J. Am. Chem. Soc.*, 2005, **127**, 3100.
34 (*a*) K. J. Haack, S. Hashiguchi, A. Fujii, T. Ikariya and R. Noyori, *Angew. Chem., Int. Ed. Engl.*, 1997, **36**, 285; (*b*) C. A. Sandoval, T. Ohkuma, N. Utsumi, K. Tsutsumi, K. Murata and R. Noyori, *Chem.–Asian J.*, 2006, **1**, 102; (*c*) Z. M. Heiden and T. B. Rauchfuss, *J. Am. Chem. Soc.*, 2006, **128**, 13048.
35 C. Gunanathan, B. Gnanaprakasam, M. A. Iron, L. J. W. Shimon and D. Milstein, *J. Am. Chem. Soc.*, 2010, **132**, 14763.
36 L. Polgár, *Cell. Mol. Life Sci.*, 2005, **62**, 2161.
37 For an example of the observation of hydrogen bonding between an *N*-heterocylic H-bond donor moiety (indolic NH) and basic anions by ^{1}H NMR spectroscopy, see Q. Li, Y. Guo and S. Shao, *Analyst*, 2012, **137**, 4497.

